



Cite this: DOI: 10.1039/d6cc02190e

 Received 9th April 2026,
Accepted 23rd May 2026

DOI: 10.1039/d6cc02190e

rsc.li/chemcomm

Measuring ionic conductivity in electrodes prepared by solvent-free melt extrusion

 Charlotte Sorel, Paul Nicolle, Gabrielle Foran,  Arnaud Prébé  and Mickael Dollé *

Battery electrodes must simultaneously conduct electrons and ions to enable charge transfer to take place. Conductivity is conferred using a combination of ion-conducting polymeric binder material and electronically conductive carbon. This work presents a reproducible technique for measuring the ionic conductivity of electrodes made from formulations containing thermoplastic vulcanizates.

One of the most common strategies to isolate the ionic conductivity in electrodes is the use of electronically insulating layers. Such stacks have previously been used to quantify ionic conductivity in electrodes for lithium-ion batteries. These electrodes are prepared by solution casting and are comprised of large amounts of active material coupled with small quantities of conductive carbon additives and polymeric binder. Some examples include Zahnow *et al.* who prepared a ceramic-based lithium phosphate-NMC(LiNi_{0.33}Mn_{0.33}Co_{0.33}O₂)-lithium phosphate stack, Siroma *et al.* who used a Li₂S-P₂S₂-based stack to measure ionic conductivity in both NMC and graphite electrodes and Asano *et al.* who used a stack comprised of NMC sandwiched between two Li₃PS₄ electrodes.^{1–3} The ceramic to solution-casted electrode interfaces in these systems can lead to significant limitations in electrical characterization because voids, cracks and grain boundaries can impact the mechanism of ionic conductivity and other electrochemical phenomena at the electrolyte–electrode interface.⁴

Challenges related to interfacial contact can be mitigated by using either solution- or polymer-based electrodes and/or electrolytes in these stacks. For example, Mourshed *et al.* measured the ionic conductivity of a carbon-based slurry electrode between two metallic plates.⁵ Orikasa *et al.* used a polypropylene-LFP(LiFePO₄)-polypropylene stack to determine the ionic conductivity of a LFP electrode.⁶ Ionic conductivities in polymer electrolyte membranes for fuel cells were analyzed in stacks based on Nafion membranes.^{7,8} These strategies were considered here where a

polymer stack was devised to measure ionic conductivity in composite electrodes prepared *via* solvent-free melt extrusion.

Composite electrodes comprised of an active material, either carbon black or a mixture of carbon black and carbon nanofibers and a thermoplastic vulcanizate (TPV) electrolyte were prepared. TPV electrolytes are made *via* the dynamic vulcanization of an elastomeric phase in a conductive thermoplastic phase.^{9,10} The inclusion of a thermoplastic phase means that TPV electrolytes can be reprocessed, allowing for the incorporation of solid powders such as active material and conductive carbon.⁹ Preliminary cycling tests with TPV electrolytes comprised of polycaprolactone (PCL) and hydrogenated nitrile butadiene rubber (HNBR) showed that electrodes made from these materials can be cycled with both LFP and NMC but further optimization is required.¹¹

TPV electrolytes comprised of PCL and EPDM (ethylene propylene diene monomer) are presented in this work. EPDM was used as the elastomeric phase because the PCL-EPDM electrolyte has higher ionic conductivity than the PCL-HNBR analogue. Further electrode optimization is possible *via* changes in the quantity and type of active material and conductive carbon used.¹² The original formulation was comprised of 60 wt% active material, 26 wt% polymeric binder and 14 wt% conductive carbon.¹¹ As increased active material content is linked to improved energy density,¹² electrode formulations with up to 75 wt% NMC were prepared (Table 1).

Interfacial contact can be optimized in a stack where all layers are prepared using the same polymer. This improves connectivity and adhesion while limiting void formation, interfacial resistance and polarization issues. This is not feasible with the PVDF/CMC-based electrodes that are used in lithium-ion batteries. Melt-processed electrodes tend to have no/low porosity. Therefore, decreases in ionic conductivity related to porosity as observed by Zahnow *et al.*,¹ are not expected to have a large impact on the measured values.

Stacks consisting of a composite electrode centered between two TPV polymer electrolytes of known ionic conductivity were developed. The TPV electrolytes act as electronic insulators

Université de Montréal, 1375 avenue Thérèse-Lavoie-Roux, Montréal, Québec, Canada H2V 0B3. E-mail: mickael.dolle@umontreal.ca



Table 1 Electrode formulations

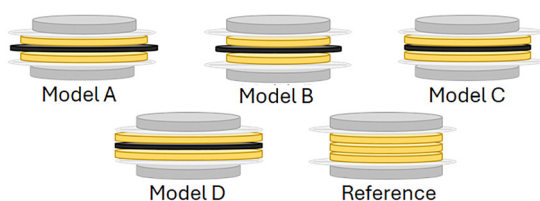
Electrode	Polymer wt%	Polymer vol%	AM wt%	CB wt%	CNF wt%
PCL-EPDM-1	26	56	NMC 60	14	
PCL-EPDM-2	26	56	NMC 60	9.8	4.2
PCL-EPDM-3	26	51	LFP 60	14	
PCL-EPDM-4	26	51	LFP 60	9.8	4.2
PCL-EPDM-5	20	52	NMC 75	5	
PCL-EPDM-6	20	52	NMC 75	3.5	1.5
PCL-EPDM-7	15	41	NMC 75	10	
PCL-EPDM-8	15	41	NMC 75	7	3

AM = active material, CB = carbon black, CNF = carbon nanofiber.

allowing only the ionic conductivity of the cathode to be measured. The contributions of the electrolytes is subtracted from the total ionic conductivity to obtain that of the electrode. Ionic conductivity testing was done on each model to determine how the respective diameters of the electrolyte and electrode layers impact accuracy (Fig. 1).

Models were tested by measuring the ionic conductivity of a PCL-HNBR TPV electrolyte and compared to a reference (Fig. 2). Measurements were performed using two different instruments: the MTZ-35 and SP-300, both from Biologic. The use of both instruments demonstrates the reproducibility of the method. The ionic conductivity of the reference at 60 °C was $1.93 \times 10^{-5} \text{ S cm}^{-1}$ with a standard deviation of $2 \times 10^{-6} \text{ S cm}^{-1}$.

Fig. 2 shows that model C yielded the most constant conductivity values for the reference sample on both instruments. The final setup therefore consists of an 18 mm electrode disk sandwiched between two 18 mm electrolyte disks (Model C, Fig. 1). The polymer-based stack is placed between two Mylar rings with an outer diameter of 19 mm and an inner diameter of 12 mm. Mylar is an insulating material that was added to reduce the risk of short circuiting and prevent ionic conductivity between the electrolyte layers, circumventing the electrode. The 12 mm diameter was used to calculate the cross-sectional



Model	A	B	C
TPV Electrolyte Diameter (mm)	18	16	18
Electrode Diameter (mm)	20	18	18
Model	D	Reference	
TPV Electrolyte Diameter (mm)	20	16	
Electrode Diameter (mm)	20	/	

Fig. 1 Model TPV electrolyte–electrode–TPV electrolyte stacks used to measure electrode ionic conductivity.

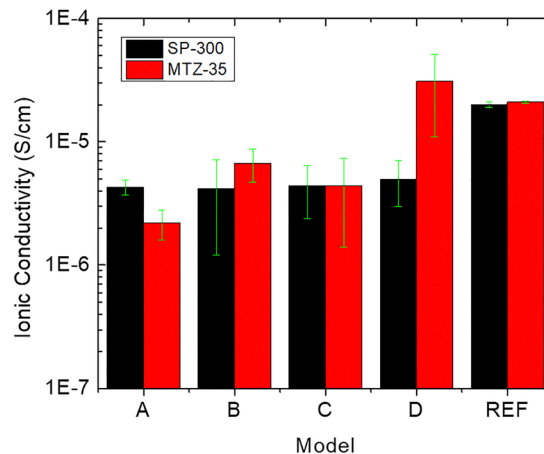


Fig. 2 Comparison between ionic conductivities of the PCL-HNBR TPV electrolyte measured at 60 °C using models A through D with the SP-300 and the MTZ-35.

area for the impedance measurement. The remaining edge was blocked on both sides by mylar which is ionically and electronically insulating, preventing parasitic impedance pathways. The chosen configuration had an average error of 5% when used with the SP-300.

The resultant Nyquist plot, which is comprised of resistances corresponding to both TPV electrolyte layers and the electrode (R_2), was fit with an equivalent circuit (Fig. 3). The equivalent circuit includes an induction loop (L_1) to account for induction behaviour at high frequencies caused by the potentiostat wiring, a resistor (R_1) to account for the resistance of the instrument (about 20Ω in Fig. 3) and constant phase elements (Q_2) and (Q_3) that represent diffusion. An R/C circuit, as opposed to the transmission line model, was used since the relative absence of porosity, lack of ion transfer to ionically insulating active materials and the use of a PCL-EPDM electrolyte as electronically insulating layers allow the system to be simplified to include bulk electrolyte resistance only.^{6,13} This equivalent circuit was previously used to isolate fluorine ion conductivity in ceramic electrodes but is used here

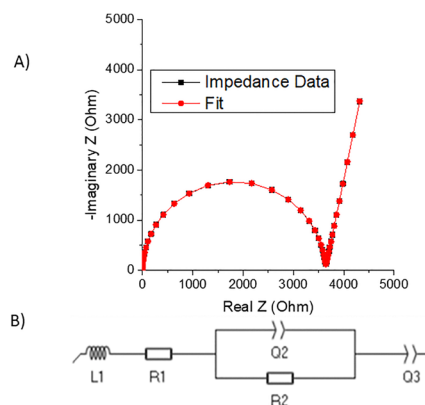


Fig. 3 (A) Nyquist plot obtained when measuring the ionic conductivity of a PCL-HNBR TPV electrolyte using the Model C stack illustrated in Fig. 1. (B) Equivalent circuit model used to extract individual contributions from the total ionic conductivity.



for solid polymer electrodes for the first time.¹⁴ TPV electrolyte resistance was determined based on the known conductivity of the reference and the thickness of the layers. This was subtracted from the total resistance to obtain the contribution of the electrode. Electrolyte and electrode layer thicknesses were measured using an optical microscope. Fitting parameter values for samples PCL-EPDM-1 through PCL-EPDM-4 can be found in Table S1.

The inclusion of active material and conductive carbon should decrease the ionic conductivity of the electrode with respect to that of the PCL-EPDM electrolyte due to increased tortuosity in the material. The ionic conductivity of the TPV electrolyte is $3.07 \times 10^{-5} \text{ S cm}^{-1}$ at 60 °C. This is about an order of magnitude higher than the ionic conductivities of the electrodes with either 60 or 75 wt% active material (Fig. 4).

A higher proportion of ionically conductive polymer makes the electrodes that contain 60 wt% active material more conductive (Fig. 4). Experimentally measured water content was 1000 to 2000 ppm for all samples and was not deemed to contribute significantly to the observed differences in ionic conductivity, as previously observed in solid polymer electrolytes by Caradant *et al.*¹⁵ Samples with 60 wt% active material that contained carbon nanofibers were slightly more conductive than those that did not (Fig. 4). The larger size of the carbon nanofibers relative to carbon black is thought to be responsible for the differences in ionic conductivity between the nanofiber and non-nanofiber formulations. There is not a significant difference in ionic conductivity between samples prepared with

NMC and those prepared with LFP despite the NMC samples containing 5 vol% more polymeric binder (Fig. 4).

Ionic conductivities were lower in formulations that contained 75 wt% active material. PCL-EPDM-5 and PCL-EPDM-6 contained 52 vol% PCL-EPDM whereas PCL-EPDM-7 and PCL-EPDM-8 contained 41 vol% polymer (Table 1). Surprisingly, the reduction in ionic conductivity in EPDM-6 and EPDM-8 seemed to be linked to the presence of carbon nanofibers, unlike the formulations with 60 wt% active material. Higher ionic conductivity in PCL-EPDM-7 and PCL-EPDM-8 than in PCL-EPDM-5 and PCL-EPDM-6 was unexpected as the volumetric proportion of the conductive polymeric phase was higher in PCL-EPDM-5 and PCL-EPDM-6. This suggests that the distribution of active material and conductive carbon in the electrodes may have a more significant impact on long-range ion transfer than total polymer content.

Reported ionic conductivities were investigated on the grounds of tortuosity (τ) (Fig. 5), as calculated based on eqn (1). Where the TPV electrolyte is the conductive phase. Volume percentage of the conductive phase (ε) is given in Table 1. The polymer volumes used to calculate tortuosity were decreased in accordance with measured sample density (Table S2) for the electrodes that contained 75 wt% NMC. σ_{opt} is the known ionic conductivity of the TPV electrolyte at 60 °C and σ_{exp} is the measured ionic conductivity of the electrode at 60 °C.

$$\tau = \frac{\varepsilon \times \sigma_{\text{opt}}}{\sigma_{\text{exp}}} \quad (1)$$

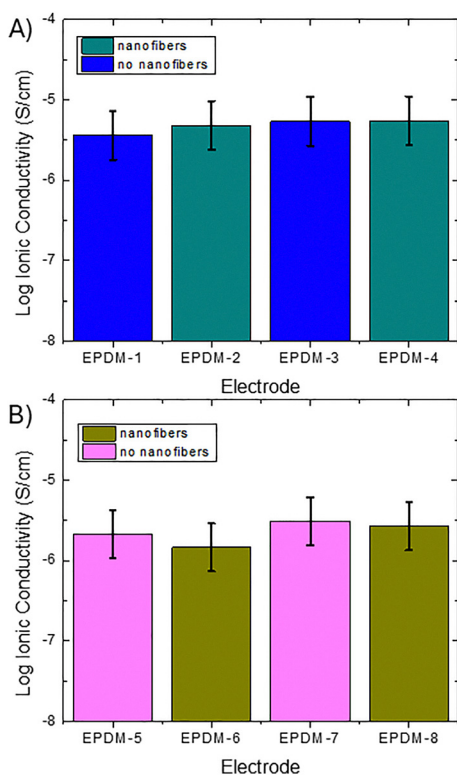


Fig. 4 (A) Ionic conductivity of PCL-EPDM based electrodes prepared with 60 wt% active material. (B) Ionic conductivity of PCL-EPDM based electrodes prepared with 75 wt% active material.

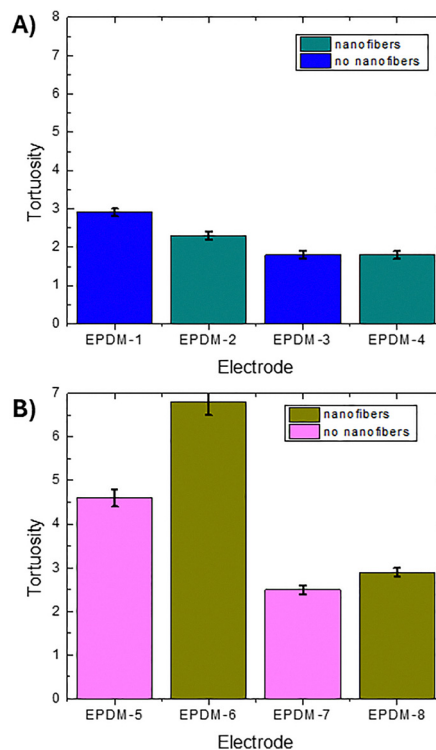


Fig. 5 (A) Tortuosity of PCL-EPDM based electrodes prepared with 60 wt% active material. (B) Tortuosity of PCL-EPDM based electrodes prepared with 75 wt% active material.



Tortuosity is a measure of the non-uniformity of the solid electrolyte in the composite electrode.³ This parameter ranged from 1.8 to 6.7 (Fig. 5). This is comparable to the tortuosity of 4 to 6 that was observed in composite electrodes containing 48 to 62 vol% NMC by Asano *et al.*³ Differences in tortuosity were attributed to differences in active material and conductive carbon content and the distribution of these materials in the polymer matrix due to no/minimal porosity. Fig. 5 shows that tortuosity was higher in the electrodes that contain 75 wt% NMC. This was expected due to a higher proportion of active material being present to disrupt the conductive polymer network. Tortuosity in the samples prepared with 60 wt% active material was higher in those that contained NMC with the NMC sample without carbon nanofibers being the most tortuous. The presence of nanofibers slightly increased the tortuosity of the LFP-containing sample. Increased tortuosity was observed for the 75 wt% NMC samples that contained carbon nanofibers, correlating with decreased ionic conductivity. Differences in tortuosity between samples with and without carbon nanofibers were attributed to differences in packing density between carbon nanofibers and carbon black. Carbon nanofibers have previously been shown to disrupt ionic conductivity through the polymer matrix by impeding polymer chain mobility in amorphous regions.¹⁶ Activation energies were calculated based on ionic conductivities between 40 and 80 °C. Activation energies depended only on the presence of carbon nanofibers (Table S3 and Fig. S1), suggesting that the absence of carbon nanofibers impacts ion mobility in the PCL-EPDM polymer matrix.

It was concluded that the polymer-based electrolyte–electrode–electrolyte stack presented here can be used to accurately measure the ionic conductivity of melt-processed solid polymer electrodes containing active material and conductive carbon. Errors in ionic conductivity were about 5% when compared to a stack comprised of three pieces of melt-processed electrolyte with known conductivity. The primary advantage of this assembly over those presented in previous publications is that all components of the stack are prepared without added solvents, thus simplifying sample preparation and removing the impact of added solvents on the ionic conductivity of polymer electrolytes.^{17,18} The use of the same polymeric phase in the electrolyte layers and as a binder material for the electrolyte is expected to provide good interfacial connectivity between layers, limiting barriers to ionic conductivity measurement such as interface incompatibility and stack polarization due to differences in ion diffusion between layers. The assembly is versatile as any ionically conductive polymer (or blends of polymers) that is compatible with melt processing can be used to construct the electrode and the stack. Decreasing the proportion of conductive polymer in the electrode lowered ionic conductivity. The presence/absence of carbon nanofibers had limited impact on the measured conductivities despite generally resulting in increased tortuosity. This observation was associated with the high packing density of carbon black.

Conflicts of interest

There are no conflicts to declare.

Data availability

The data supporting this article including experimental information, Nyquist plot fits, density calculations and activation energy plots have been included as part of the supporting information (SI). See DOI: <https://doi.org/10.1039/d6cc02190e>.

Acknowledgements

The authors would like to acknowledge financial support received from the Natural Sciences and Engineering Research Council of Canada and TotalEnergies (NSERC RDCPJ 528052-18).

References

- J. Zahnow, T. Bernges, A. Wagner, N. Bohn, J. R. Binder, W. G. Zeier, M. T. Elm and J. Janek, Impedance Analysis of NCM Cathode Materials: Electronic and Ionic Partial Conductivities and the Influence of Microstructure, *ACS Appl. Energy Mater.*, 2021, **4**, 1335–1345.
- Z. Siroma, T. Sato, T. Takeuchi, R. Nagai, A. Ota and T. Ioroi, AC impedance analysis of ionic and electronic conductivities in electrode mixture layers for an all-solid-state lithium-ion battery, *J. Power Sources*, 2016, **316**, 215–223.
- T. Asano, S. Yubuchi, A. Sakuda, A. Hayashi and M. Tatsumisago, Electronic and Ionic Conductivities of $\text{LiNi}_{1/3}\text{Mn}_{1/3}\text{Co}_{1/3}\text{O}_2\text{-Li}_3\text{PS}_4$ Positive Composite Electrodes for All-Solid-State Lithium Batteries, *J. Electrochem. Soc.*, 2017, **164**, A3960–A3963.
- A. Orue Mendizabal, M. Cheddadi, A. Tron, A. Beutl and P. López-Aranguren, Understanding Interfaces at the Positive and Negative Electrodes on Sulfide-Based Solid-State Batteries, *ACS Appl. Energy Mater.*, 2023, **6**, 11030–11042.
- M. Mourshed, S. M. Rezaei Niya and B. Shabani, Experimental Study of Electronic and Ionic Conductivity of a Carbon-Based Slurry Electrode Used in Advanced Electrochemical Energy Systems, *ACS Appl. Energy Mater.*, 2022, **5**, 11413–11430.
- Y. Orikasa, Y. Gogyo, H. Yamashige, M. Katayama, K. Chen, T. Mori, K. Yamamoto, T. Masese, Y. Inada, T. Ohta, Z. Siroma, S. Kato, H. Kinoshita, H. Arai, Z. Ogumi and Y. Uchimoto, Ionic conduction in lithium ion battery composite electrode governs cross-sectional reaction distribution, *Sci. Rep.*, 2016, **6**, 2–7.
- J. A. Shetline and S. E. Creager, Quantifying Electronic and Ionic Conductivity Contributions in Carbon/Polyelectrolyte Composite Thin Films, *J. Electrochem. Soc.*, 2014, **161**, H917–H923.
- S. Y. An, B. T. McAllister, E. Grignon, S. Evariste and D. S. Seferos, Increasing ionic conductivity in polymer electrolytes using oxanorbornene, *EcoMat*, 2022, **4**, 1–9.
- N. Ning, S. Li, H. Wu, H. Tian, P. Yao, G. H. Hu, M. Tian and L. Zhang, Preparation, microstructure, and microstructure-properties relationship of thermoplastic vulcanizates (TPVs): A review, *Prog. Polym. Sci.*, 2018, **79**, 61–97.
- T. Chatterjee, D. Basu, A. Das, S. Wiessner, K. Naskar and G. Heinrich, Super thermoplastic vulcanizates based on carboxylated acrylonitrile butadiene rubber (XNBR) and polyamide (PA12), *Eur. Polym. J.*, 2016, **78**, 235–252.
- L. Caradant, G. Foran, D. Lepage, P. Nicolle, A. Prébé, D. Aymé-Perrot and M. Dollé, Harnessing melt processing for the preparation of mechanically robust thermoplastic vulcanizate electrolytes, *J. Power Sources Adv.*, 2024, **28**, 100149.
- W. Mei, H. Chen, J. Sun and Q. Wang, The effect of electrode design parameters on battery performance and optimization of electrode thickness based on the electrochemical-thermal coupling model, *Sustainable Energy Fuels*, 2019, **3**, 148–165.
- P. Braun, C. Uhlmann, M. Weiss, A. Weber and E. Ivers-Tiffée, Assessment of all-solid-state lithium-ion batteries, *J. Power Sources*, 2018, **393**, 119–127.
- A. Grenier, A. G. Porras-Gutierrez, M. Body, C. Legein, F. Chrétien, E. Raymundo-Piñero, M. Dollé, H. Groult and D. Dambournet, Solid Fluoride Electrolytes and Their Composite with Carbon: Issues and Challenges for Rechargeable Solid State Fluoride-Ion Batteries, *J. Phys. Chem. C*, 2017, **121**, 24962–24970.



- 15 L. Caradant, N. Verdier, G. Foran, D. Lepage, A. Prébé, D. Aymé-Perrot and M. Dollé, Extrusion of Polymer Blend Electrolytes for Solid-State Lithium Batteries: A Study of Polar Functional Groups, *ACS Appl. Polym. Mater.*, 2021, **3**, 6694–6704.
- 16 P. Pötschke, M. Abdel-Goad, I. Alig, S. Dudkin and D. Lellinger, Rheological and dielectrical characterization of melt mixed polycarbonate-multiwalled carbon nanotube composites, *Polymer*, 2004, **45**, 8863–8870.
- 17 D. Mankovsky, D. Lepage, M. Lachal, L. Caradant, D. Aymé-Perrot and M. Dollé, Water Content in Solid Polymer Electrolytes: The Lost Knowledge, *Chem. Commun.*, 2020, **56**, 10167–10170.
- 18 G. Foran, D. Mankovsky, N. Verdier, D. Lepage, A. Prébé, D. Aymé-Perrot and M. Dollé, The Impact of Absorbed Solvent on the Performance of Solid Polymer Electrolytes for Use in Solid-State Lithium Batteries, *iScience*, 2020, **23**, 101597.

